

Diffraction of helical x-rays by optically active achiral crystals

S. W. Lovesey 

ISIS Facility, STFC, Didcot, Oxfordshire OX11 0QX, United Kingdom
and Diamond Light Source Ltd, Didcot, Oxfordshire OX11 0DE, United Kingdom



(Received 24 September 2021; accepted 22 November 2021; published 3 December 2021)

Four crystal classes are optically active yet not chiral (nonenantiomorphic). Corresponding Bragg diffraction patterns calculated for circularly polarized (helical) x-rays tuned to an atomic resonance display angular anisotropy in the distribution of electrons at spots not indexed on the chemical structure (defined by a space group derived from Thomson scattering by perfect spheres of charge). Templeton-Templeton scattering, as it is usually called, of helical x-rays is quantified in terms of a chiral signature defined as the partial diffracted intensity hallmarked by x-ray helicity. Our electric dipole-electric dipole (E1-E1) chiral signature for a space group in the optically active crystal class $\bar{4}2m$ (D_{2d}) affords a complete interpretation in terms of copper quadrupoles of diffraction data collected on copper metaborate [Ovchinnikova *et al.*, *J. Synchrotron Radiat.* **28**, 1455 (2021)]. An example of a chiral signature derived from a parity-odd resonance event (E1-E2) is included in our study. It is firmly established that tuning the energy of x-rays to an atomic resonance enhances the intensity of inherently weak Templeton-Templeton scattering and renders space-group forbidden Bragg spots element specific. Our chiral signature as a function of rotation about the reflection vector (azimuthal-angle scan) is specific to position multiplicity, Wyckoff letter and symmetry in a favorable space group.

DOI: [10.1103/PhysRevB.104.235106](https://doi.org/10.1103/PhysRevB.104.235106)

I. INTRODUCTION

J. Willard Gibbs, best known for pioneer work on statistical mechanics perhaps, used Maxwell's equations of electrodynamics in a demonstration that certain crystals can be both optically active (rotation of the plane of polarization of light) and achiral (nonenantiomorphic) [1]. Different theory, based on a pseudotensor of rank 2, was adopted in subsequent work which established that crystal classes m (C_s), $mm2$ (C_{2v}), $\bar{4}$ (S_4), and $\bar{4}2m$ (D_{2d}) possess the dual properties; see, for example, Refs. [2,3]. The pseudotensor is certainly zero for materials that possess a center of inversion symmetry. It can be different from zero for 11 enantiomorphic crystal classes (absence of both a center and a plane of symmetry), and the named four nonenantiomorphic classes that are identical to their mirror images. Optical experiments on crystal types $\bar{4}2m$ (silver thiogallate) and $\bar{4}$ (cadmium gallium sulphide) by Hobden published between 1967 and 1969 confirmed that nonenantiomorphic crystals can present optical rotation or gyration, as it is sometimes known [4–7]. The crystals show birefringence (double refraction) that overwhelms optical activity. At specific wavelengths, the crystals are accidentally isotropic, however, which allowed Hobden to study optical activity without the difficulties arising from the presence of birefringence.

Coupling of helicity in a beam of x-rays and a crystal chiral axis has been confirmed in diffraction by several enantiomorphic materials [8–13], together with imaging the chirality of domains in racemic twinned Cs Cu Cl₃ [14]. Weak Bragg spots not indexed on the chemical crystal structure are created by angular anisotropy in the distribution of atomic electrons. It

is often referred to as Templeton-Templeton scattering (T&T) after the pioneers [15,16]. Signal enhancement is gained by tuning the energy of primary photons to an atomic resonance, which adds specification of an element to the desirable features of the x-ray diffraction technique. To date, there are successful experiments on low quartz, tellurium, and berillite (Al P O₄) with enantiomorphs that belong to trigonal $P3_121$ (right-handed screw) and $P3_221$ (left-handed screw), and resonant ions occupy sites with multiplicity three [8–13]. Diffraction patterns and azimuthal-angle scans (rotation of the diffracting crystal about the axis of the reflection vector) were measured with the energy of primary x-rays tuned to K edges ($1s$) of Si and Al, for example.

We investigate Bragg diffraction of circularly polarized x-rays by crystal classes C_s , C_{2v} , S_4 , and D_{2d} , and thereby extend our understanding of what can be learned from appropriate experiments. Calculated scattering amplitudes account for the enhancement of Bragg spots by an atomic resonance and a rotation of the crystal about the reflection vector. Use is made of a chiral signature Υ specific to position multiplicity, Wyckoff letter, and symmetry in a space group. Our findings imply a universal azimuthal-angle dependence of Υ in diffraction enhanced by electric dipole-electric dipole (E1-E1) and electric dipole-electric quadrupole (E1-E2) absorption events. The signal is absent for the four space groups in the C_s crystal class, and the two space groups in S_4 . By way of an example, copper and neodymium ions in the one-dimensional type cuprate Nd₂Ba₄Cu₂O₉ occupy sites $4f$ in the tetragonal space group $P\bar{4}n2$ in crystal class D_{2d} . Their contributions to a Bragg diffraction pattern are specified by the energy of the chosen

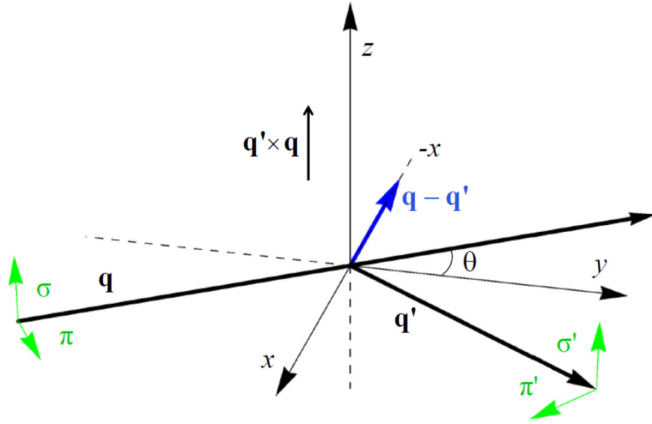


FIG. 1. Primary (σ, π) and secondary (σ', π') states of polarization. Corresponding wave vectors \mathbf{q} and \mathbf{q}' subtend an angle 2θ , and the reflection vector $\boldsymbol{\kappa} = \mathbf{q} - \mathbf{q}'$.

atomic resonance, and specific electronic structures that create quadrupoles and the chiral signature.

II. RESONANT SCATTERING

The nature of the electronic ground state accessed in resonant diffraction depends on both the quantum labels of the virtual, intermediate state and the type of the absorption event, whose actual strength may depend on its energy. An E1 event and absorption of hard x-rays (energy $E \approx 5\text{--}9\text{ keV}$) at a K edge can access p -like atomic states, while an E2 event can access d -like states. Levels of enhancement are very small set against factors enjoyed at actinide $M_{4,5}$ absorption edges. Direct access with an E1 event to d -like states is allowed by absorption at L edges, and an even larger enhancement is expected. It can even be comparable to the intensities of Thomson reflections from the chemical structure. Not all crystal structures satisfy the Laue condition for Bragg diffraction with an x-ray wavelength $\approx (12.4/E)\text{ \AA}$ and E in units of keV.

Assuming that virtual intermediate states are spherically symmetric, to a good approximation, the x-ray scattering length $\approx \{F_{\mu\eta}/(E - \Delta + i\Gamma/2)\}$ in the region of the resonance, where Γ is the total width of the resonance at an energy Δ [10,17–19]. The numerator $F_{\mu\eta}$ is an amplitude, or unit-cell structure factor, for Bragg diffraction in the scattering channel with primary (secondary) polarization $\eta(\mu)$. By convention, σ denotes polarization normal to the plane of scattering, and π denotes polarization within the plane of scattering. Figure 1 depicts polarization states, wave vectors, and the Bragg condition.

III. CHIRAL SIGNATURE

Photon and electronic quantities in the scattering amplitude are partitioned in a generalized scalar product $F_{\mu\eta} = \{\mathbf{X}^K \bullet \langle \mathbf{O}^K \rangle\}$, with implied sums on rank K and associated projections Q in the interval $-K \leq Q \leq K$ [18,19]. Angular brackets about the atomic tensor operator O^K_Q in an electronic multipole $\langle O^K_Q \rangle$ denote its time average, or expectation value. Selection rules on K and Q for the multipole imposed by symmetry of the site used by the resonant ion are evidently

duplicated in the x-ray factor \mathbf{X}^K . The latter is specific to a resonant event. One finds \mathbf{X}^K is independent of photon wave vectors for an E1-E1 event ($K = 0\text{--}2$) but this is not so for E1-E2 ($K = 1\text{--}3$) and E2-E2 ($K = 0\text{--}4$) absorption events. All information on x-ray factors needed here is found in Refs. [18,19]. Electronic multipoles can be calculated using standard tools of atomic physics given a suitable wave function [9]. Alternatively, multipoles can be estimated from a tried and tested simulation program of electronic structure [10]. The complex conjugate of an atomic multipole $\langle O^K_Q \rangle^* = (-1)^Q \langle O^{K-Q} \rangle$, with a phase convention $\langle O^K_Q \rangle = [\langle O^K_Q \rangle' + i\langle O^K_Q \rangle'']$ for real and imaginary parts labeled by single and double primes, respectively.

Henceforth, we adopt a shorthand $(\mu\eta)$ for the scattering amplitude $F_{\mu\eta}$. Scattered intensity picked out by circular polarization in the primary photon beam = $P_2\Upsilon$,

$$\Upsilon = \{(\sigma'\pi)^*(\sigma'\sigma) + (\pi'\pi')^*(\pi'\sigma)\}'', \quad (1)$$

and the Stokes parameter P_2 (a purely real pseudoscalar) measures helicity in the primary x-ray beam; cf. Eq. (12) in Ref. [10]. Since intensity is a scalar quantity, Υ and P_2 must possess identical discrete symmetries, specifically, both scalars are time even and parity odd. The signature Υ is extracted from observed intensities by subtraction of intensities measured with opposite-handed primary x-rays, namely, $\pm P_2$. Intensity of a Bragg spot in the rotated channel of polarization is proportional to $|(\pi'\sigma)|^2$, and likewise for unrotated channels of polarization.

We use $\Psi^K_Q = [\exp(i\boldsymbol{\kappa} \bullet \mathbf{d})\langle O^K_Q \rangle_{\mathbf{d}}]$ for an electronic structure factor, where the reflection vector $\boldsymbol{\kappa}$ is defined by integer Miller indices (h, k, l) , and the implied sum in Ψ^K_Q is over all sites \mathbf{d} in a unit cell used by resonant ions. Construction of Ψ^K_Q requires symmetry operators for a space group together with the symmetry of occupied sites. All necessary information is available on the Bilbao server [20]. The four amplitudes required in the chiral signature defined in Eq. (1) are derived from Ψ^K_Q and universal expressions for E1-E1 and E1-E2 scattering amplitudes [19].

IV. OPTICALLY ACTIVE ACHIRAL SPACE GROUPS

Calculations return null chiral signatures for crystal classes C_s and S_4 . For the two remaining optically active achiral space groups our goal is to raise awareness of the virtue of the chiral signature. Many real samples have been identified [21], and likely more wait to be discovered, and it is not prudent to attempt construction of a catalog of materials.

A. C_{2v}

There are 22 space groups in the orthorhombic crystal class $mm2$ (C_{2v}), with cell lengths $a \neq b \neq c$. Space group $Pca2_1$ (No. 29) is chosen as an opening illustration because it consists of sites $4a$ alone. Sites have no symmetry. In consequence, projections Q in the interval $-K \leq Q \leq K$ for a multipole $\langle O^K_Q \rangle$ are unrestricted. The electronic structure factor is

$$\begin{aligned} \Psi^K_Q(4a) &= \langle O^K_Q \rangle [\exp(i\delta) + (-1)^{Q+l} \exp(-i\delta)] \quad (\text{No. 29}) \end{aligned}$$

$$+ \sigma_\pi \langle O^K_Q \rangle^* (-1)^{K+h} \times [\exp(i\chi) + (-1)^{Q+l} \exp(-i\chi)], \quad (2)$$

where $\delta = 2\pi(xh + yk)$, $\chi = 2\pi(xh - yk)$, and x and y are general coordinates. The parity signature $\sigma_\pi = +1(-1)$ for a parity-even (parity-odd) absorption event, e.g., E1-E1 (E1-E2). Examination of $\Psi^K_0(4a)$ with K even and $\sigma_\pi = +1$ reveals that reflections $(h, 0, 0)$ and $(0, k, l)$ with Miller indices h and l odd, respectively, are not indexed on the crystal structure, i.e., $\Psi^K_0(4a)$ is zero for said conditions. T&T scattering at such Bragg spots is created by nondiagonal multipoles with projections $|Q| > 0$.

We proceed with a study of $(h, 0, 0)$ and h odd utilizing the E1-E1 event. Multipoles with $\sigma_\pi = +1$ are denoted $\langle T^K_Q \rangle$. Let the two quantities $A = -4\sin(\varphi_h)\langle T^2_{+1} \rangle''$ and $B = 4i\cos(\varphi_h)\langle T^2_{+2} \rangle''$ in which $\delta = \chi = \varphi_h = 2\pi xh$. Scattering amplitudes are [19]

$$\begin{aligned} (\sigma'\sigma) &= -i\sin(2\psi)A, & (\pi'\pi) &= \sin^2(\theta)(\sigma'\sigma), \\ (\pi'\sigma) &= -i\sin(\theta)\cos(2\psi)A + i\cos(\theta)\sin(\psi)B, \\ & & (2m+1, 0, 0; \text{No. 29}) & \end{aligned} \quad (3)$$

and $(\sigma'\pi)$ is derived from $(\pi'\sigma)$ by a change in sign to A . The Bragg angle θ is defined in Fig. 1. Note that amplitudes $(\sigma'\sigma)$ and $(\pi'\pi)$ are purely imaginary, while $(\sigma'\pi)$ and $(\pi'\sigma)$

are complex. The azimuthal angle ψ measures rotation of the crystal about the reflection vector, and the crystal b axis is in the plane of scattering for $\psi = 0$. It follows that the chiral signature of the Bragg spot $(h, 0, 0)$ enhanced by an E1-E1 absorption event is

$$\Upsilon_+(4a) = -8\Phi(\varphi_h, \psi)\langle T^2_{+1} \rangle''\langle T^2_{+2} \rangle'', \quad (2m+1, 0, 0; \text{No. 29}), \quad (4)$$

where

$$\Phi(\varphi_h, \psi) = \cos^3(\theta)\sin(2\varphi_h)\sin(\psi)\sin(2\psi). \quad (5)$$

The azimuthal-angle dependence captured in $\Phi(\varphi_h, \psi)$ appears to be universal to E1-E1 and E1-E2 absorption events. The two multipoles that create Υ have angular characters (yz) and (xy) . Dependence of Υ on $\varphi_h = 2\pi xh$ will likely generate optimal chiral signatures at particular Bragg spots. The subscript on $\Upsilon_+(4a)$ denotes the fact that the parity signature $\sigma_\pi = +1$.

The fundamental structure of $\Upsilon_-(4a)$ for an E1-E2 event is similar to $\Upsilon_+(4a)$. The number of multipoles engaged is the defining difference, and it arises from the fact that polar multipoles $\langle U^K_Q \rangle$ have ranks $K = 1, 2$, and 3 and projections Q are unrestricted by site symmetry. Scattering amplitudes in unrotated channels of polarization are purely imaginary. Amplitudes in rotated channels are complex, and their real parts allow $\Upsilon_-(4a)$ different from zero. For E1-E2 we find

$$\begin{aligned} \Upsilon_-(4a) &= (16/(15\sqrt{5}))\sin^2(\theta)\Phi(\varphi_h, \psi)[3\langle U^1_{+1} \rangle'' + 2\sqrt{5}\langle U^2_{+1} \rangle' - \langle U^3_{+1} \rangle'' + \sqrt{15}\langle U^3_{+3} \rangle''] \\ &\times [\sqrt{6}\langle U^2_0 \rangle + \langle U^2_{+2} \rangle' + \sqrt{2}\langle U^3_{+2} \rangle''] \quad (2m+1, 0, 0; \text{No. 29}). \end{aligned} \quad (6)$$

Notably, $\Upsilon_+(4a)$ and $\Upsilon_-(4a)$ have exactly the same dependence on the azimuthal angle. Also, both chiral signatures are created by the interference of multipoles with even and odd projections.

Space group $Pna2_1$ (No. 33) likewise comprises sites $4a$ alone that have no symmetry. Reflections $(0, k, l)$ with $k + l$ odd are space-group forbidden, and $\Upsilon_+(4a) \propto [\langle T^2_{+1} \rangle'\langle T^2_{+2} \rangle'']$ for an E1-E1 absorption event.

A more typical structure comprises sites with more than one multiplicity. There are four sites with multiplicity 2 in space group $Pcc2$ (No. 27). All have site symmetry 2_z . The latter restricts projections to $Q = \pm 2n$, including $Q = 0$. Diagonal components ($Q = 0$) of the electronic structure factor, by definition, are zero at space-group forbidden reflections. Quadrupoles in T&T scattering are $\langle T^2_{\pm 2} \rangle$ at sites with 2_z symmetry. In consequence, the chiral signature is zero for such high-symmetry sites since it relies on interference between multipoles that differ by projections or ranks, or both; cf. Eq. (6).

Remaining positions $4e$ in $Pcc2$ have no symmetry. Reflections $(h, 0, l)$ and $(0, k, l)$ with l odd are forbidden. Consider the Bragg spot $(h, 0, l)$ first. Scattering amplitudes are functions of the two quantities,

$$\begin{aligned} A &= 4[p\sin(\varphi_h)\langle T^2_{+1} \rangle'' - ir\cos(\varphi_h)\langle T^2_{+2} \rangle''], \\ B &= -4[p\cos(\varphi_h)\langle T^2_{+1} \rangle'' + ir\sin(\varphi_h)\langle T^2_{+2} \rangle'']. \end{aligned} \quad (h, 0, 2m+1; \text{No. 27}) \quad (7)$$

Scattering amplitudes are derived from Eq. (3) on using these expressions. In Eq. (7), $(p, 0, r)$ is a unit vector parallel to the reflection vector, i.e., $p \propto h$ and $r \propto (al/c)$. With $\psi = 0$ and $(h, 0, 2m+1)$ the crystal b axis is in the plane of scattering, and for $(0, k, 2m+1)$ the a axis is in the plane.

Chiral signatures of the Bragg spots $(h, 0, l)$ and $(0, k, l)$ with l odd are

$$\begin{aligned} \Upsilon_+(4e) &= -8\Phi(\varphi_h, \psi)\langle T^2_{+1} \rangle''\langle T^2_{+2} \rangle'', \quad (h, 0, 2m+1; \text{No. 27}) \\ \Upsilon_+(4e) &= 8\Phi(\varphi_k, \psi)\langle T^2_{+1} \rangle'\langle T^2_{+2} \rangle''. \quad (0, k, 2m+1; \text{No. 27}) \end{aligned} \quad (8)$$

Evidently, $\Upsilon_+(4e) = 0$ for $(0, 0, 2m+1)$. Components of $\langle T^2_{+1} \rangle = [\langle T^2_{+1} \rangle' + i\langle T^2_{+1} \rangle'']$ are different at the two Bragg spots.

B. D_{2d}

Copper and neodymium ions in $\text{Nd}_2\text{Ba}_4\text{Cu}_2\text{O}_9$ occupy sites $4f$ in the tetragonal space group $P\bar{4}n2$ (No. 118) [22], with cell lengths $a = b \neq c$. Multipoles are unchanged by a dyad 2_{-xy} , and Thomson diffraction is forbidden for reflections of the type $(h, 0, 0)$ with h odd. General extinction rules for $P\bar{4}n2$ are readily derived from the electronic structure factor,

$$\begin{aligned} \Psi^K_Q(4f) = & \langle O^K_Q \rangle [\exp(i\chi) + (-1)^Q \exp(-i\chi)] \quad (\text{No. 118}) \\ & + \sigma_\pi \langle O^K_{-Q} \rangle (-1)^{K+Q} (-1)^{h+k+l} [\exp(i\delta) + (-1)^Q \exp(-i\delta)], \end{aligned} \quad (9)$$

with $x = y$ in the spatial angles χ and δ . Multipoles are obliged by site symmetry to satisfy $\langle O^K_Q \rangle = (-1)^K \exp(-i\pi Q/2) \langle O^K_{-Q} \rangle$.

Scattering amplitudes and the chiral signature for an E1-E1 event are

$$\begin{aligned} (\sigma' \sigma) = & 4i \sin(\varphi) \sin(2\psi) \langle T^2_{+1} \rangle', \quad (\pi' \pi) = \sin^2(\theta) (\sigma' \sigma), \\ (\pi' \sigma)' = & (\sigma' \pi)' = -4 \cos(\varphi) \cos(\theta) \sin(\psi) \langle T^2_{+2} \rangle'', \quad (2m+1, 0, 0; \text{No. 118}) \\ \Upsilon_+(4f) = & -8\Phi(\varphi_h, \psi) \langle T^2_{+1} \rangle' \langle T^2_{+2} \rangle'', \end{aligned} \quad (10)$$

with $\varphi_h = 2\pi xh$. General coordinates for ions using $4f$ are significantly different and mean optimal Bragg spots occur at different Miller indices h ($\text{Nd}_2\text{Ba}_4\text{Cu}_2\text{O}_9$, $x \approx 0.388$ (Nd) and 0.101 (Cu) [22]). Quadrupoles satisfy $\langle T^2_{+1} \rangle' = \langle T^2_{+1} \rangle''$.

As a second example of the crystal class type, consider space group $I\bar{4}2d$ (No. 122) with the condition $h + k + l$ even imposed on Miller indices by body centering. Compounds using this space group include Ag Ga S₂, Cu Fe S₂, and Cu B₂ O₄. Ions occupy sites with multiplicities 4 and 8. Sites $4a$, $4b$ are not of interest in the study in hand because they do not contribute T&T diffraction in E1-E1. Not so for sites $8d$ with symmetry 2_x used by S²⁻ ions in silver thiogallate and chalcopyrite, and Cu²⁺ ions in copper metaborate [23]. Reflections $(h, h, 0)$ with h odd are space-group forbidden, for example. The corresponding chiral signature $\Upsilon_+(8d)$ is the same as in Eq. (10) on replacing quadrupoles therein by $\langle T^2_{+1} \rangle''$ and $\langle T^2_{+2} \rangle'$, and multiplication by a factor $-2\sqrt{2}$. The fractional coordinate $x \approx 0.082$ for copper ions in Cu B₂ O₄ [23]. Our result $\Upsilon_+(8d)$ accounts for an azimuthal scan on the Bragg spot $h = 1$, and it specifies the nature of Cu quadrupoles exposed by helicity in the primary beam of x-rays [24].

V. DISCUSSION

An answer to the intriguing question as to whether optically active achiral crystals possess a chemical structure that interacts with helicity in a beam of x-rays is found in work reported by Ovchinnikova *et al.* [24]. The authors measured a partial intensity, defined as the difference between the intensity of Bragg spots observed with left- and right-handed x-ray, for copper metaborate with the energy of x-rays tuned to the copper K edge ($E \approx 8991$ eV, $1s \rightarrow 4p$). The material is described by one of 12 space groups in the optically active nonenantiomorphic crystal class D_{2d} .

Our calculations using C_{2v} and D_{2d} of the partial intensity, a chiral signature denoted by Υ , imply that it has a universal structure for diffraction enhanced by an electric dipole-electric dipole (E1-E1) absorption event. As a function of rotation through an azimuthal angle ψ about the reflection vector, $\Upsilon \propto \sin(\psi) \sin(2\psi)$ and, thus, zero for ψ multi-

ples of 90° , and its size and sign depend on Miller indices. As in Templeton-Templeton scattering, quadrupoles make up the electronic content of Υ , and we identify the specific quadrupoles observed in the experiment reported on Cu B₂ O₄ [24]. Multipoles are perfectly defined atomic quantities that can be calculated using a suitable electronic wave function, or calculated using a simulation of electronic structure [18,25].

Small intensity was measured ≈ 10 eV below the main intensity at an energy $E \approx 8991$ eV in the copper absorption spectrum, at which Bragg diffraction was performed [24]. A parity-odd E1-E2 absorption event is one candidate mechanism for the blip in intensity. We report a calculation of the chiral signature for E1-E2 and find it is essentially the same as for an E1-E1 event. Specifically, the azimuthal-angle dependence is the same for both absorption events. While $\Upsilon(\text{E1-E1})$ is a product of two parity-even quadrupoles with different angular anisotropies $\Upsilon(\text{E1-E2})$ can contain polar multipoles with different ranks and projections, as in the example we report, Eq. (6). We have not found $\Upsilon(\text{E1-E1})$ different from zero for chemical structures that belong to C_s and S_4 crystal classes.

A few materials that belong to crystal classes C_{2v} and D_{2d} are listed in Table I. Our chiral signature defined in Eq. (1) can be different from zero for ions using the sites mentioned. Its specific form is deduced from results presented in the main

TABLE I. Representative examples of optically active achiral materials in crystal classes C_{2v} (space groups No. 25–46, Sec. IV A) and D_{2d} (No. 111–122, Sec. IV B). Our chiral signature Υ defined in Eq. (1) can be different from zero for ions in the cited sites.

Te_2O_3 (S O ₄), $Pmn2_1$ (No. 31) sites $4b$; Te^{4+} , O^{2-} [26]
$\text{Na}_3\text{W O}_3\text{N}$, $Pmn2_1$ (No. 31) sites $4b$; Na^{1+} , O^{2-} , N^{3-} [27]
Nd Os O_4 , $Pna2_1$ (No. 33) sites $4a$; Nd^{3+} , Os^{5+} , O^{2-} [28]
$\text{Rb}_2\text{Cd Br}_2\text{I}_2$, $Ama2$ (No. 40) sites $8c$; I [29]
$\text{Ba Cu}_2\text{Sn Se}_4$, $Ama2$ (No. 40) sites $8c$; Cu, Se [30]
$\text{Nd}_2\text{Ba}_4\text{Cu}_2\text{O}_9$, $P\bar{4}n2$ (No. 118) sites $4f$; Nd^{3+} , Cu^{2+} , O^{2-} [22]
$\text{Cu B}_2\text{O}_4$, $I\bar{4}2d$ (No. 122) sites $8d$; Cu^{2+} [23]
Ag Ga S_2 , $I\bar{4}2d$ (No. 122) sites $8d$; S^{2-} [31]

text, and always it is proportional to $\Phi(\varphi, \psi)$ in Eq. (5). In the example of the tellurium sulfate [26], the signature $\Upsilon(4b)$ for space-group forbidden spots $(2m + 1, 0, 0)$ is given by Eq. (4) apart from an overall minus sign. With a cell length $a \approx 8.880 \text{ \AA}$, recovered from powder neutron diffraction patterns, the Laue condition for Bragg diffraction is not satisfied at the oxygen K edge. Absorption at the tellurium L_3 edge ($E \approx 4.345 \text{ keV}$) gives access to Bragg spots with Miller indices $h = 1, 3$, and 5 , and many more spots are accessible with absorption at the K edge ($E \approx 31.817 \text{ keV}$). From Eq. (4), $\Upsilon(4b) \propto \sin(4\pi xh)$ with $x \approx 0.301$ for tellurium, and $\sin(4\pi xh) \approx -0.935(+0.980)$ for $h = 3(7)$, while this spatial

phase factor $\approx +0.082$ for $h = 5$. Resonance-enhanced Bragg diffraction by oxygen ions can be realized with crystals of Nd Os O_4 since the cell length is much larger, $a \approx 14.859 \text{ \AA}$ [28]. Regarding the other two elements in this compound, x-rays tuned to the M_3 and M_4 edges likely yield strong enhancements, with the M_4 edge at $E \approx 1.000 \text{ keV}$ ($E \approx 2.033 \text{ keV}$) for Nd (Os).

ACKNOWLEDGMENT

Professor G. van der Laan prepared Fig. 1, and Dr. Y. Tanaka commented on the paper in its making.

-
- [1] J. W. Gibbs, *Am. J. Sci.* **23**, 460 (1882).
- [2] L. D. Landau, E. M. Lifshitz, and L. P. Pitaevskii, *Electrodynamics of Continuous Media*, 2nd ed. (Pergamon Press, Oxford, 1984).
- [3] J. F. Nye, *Physical Properties of Crystals* (Oxford University Press, London, 1964).
- [4] M. V. Hobden, *Nature (London)* **216**, 678 (1967).
- [5] M. V. Hobden, *Acta Crystallogr., Sect. A* **24**, 676 (1968).
- [6] M. V. Hobden, *Nature (London)* **220**, 781 (1968).
- [7] M. V. Hobden, *Acta Crystallogr., Sect. A* **25**, 633 (1969).
- [8] Y. Tanaka, T. Takeuchi, S. W. Lovesey, K. S. Knight, A. Chainani, Y. Takata, M. Oura, Y. Senba, H. Ohashi, and S. Shin, *Phys. Rev. Lett.* **100**, 145502 (2008).
- [9] J. Igarashi and M. Takahashi, *Phys. Rev. B* **86**, 104116 (2012).
- [10] Y. Joly, Y. Tanaka, D. Cabaret, and S. P. Collins, *Phys. Rev. B* **89**, 224108 (2014).
- [11] Y. Tanaka, T. Kojima, Y. Takata, A. Chainani, S. W. Lovesey, K. S. Knight, T. Takeuchi, M. Oura, Y. Senba, H. Ohashi, and S. Shin, *Phys. Rev. B* **81**, 144104 (2010).
- [12] Y. Tanaka *et al.*, *J. Phys.: Condens. Matter* **22**, 122201 (2010).
- [13] T. Usui, Y. Tanaka, H. Nakajima, M. Taguchi, A. Chainani, M. Oura, S. Shin, N. Katayama, H. Sawa, Y. Wakabayashi, and T. Kimura, *Nat. Mater.* **13**, 611 (2014).
- [14] H. Ohsumi *et al.*, *Angew. Chem. Int. Ed.* **52**, 8718 (2013).
- [15] D. H. Templeton, and L. K. Templeton, *Acta Crystallogr., Sect. A* **41**, 133 (1985); **A42**, 478 (1986): with a review by; V. E. Dmitrienko, K. Ishida, A. Kirfel, and E. N. Ovchinnikova, *ibid.* **A61**, 481 (2005).
- [16] D. H. Templeton, *Handbook on Synchrotron Radiation* Vol. 3, edited by G. Brown and D. E. Moncton (Elsevier Science, New York, 1991).
- [17] Ch. Brouder, *J. Phys.: Condens. Matter* **2**, 701 (1990), and copious references there in.
- [18] S. W. Lovesey, E. Balcar, K. S. Knight, and J. Fernández Rodríguez, *Phys. Rep.* **411**, 233 (2005).
- [19] V. Scagnoli and S. W. Lovesey, *Phys. Rev. B* **79**, 035111 (2009).
- [20] Bilbao crystallographic server: <http://www.cryst.ehu.es/>; S. V. Gallego *et al.*, *J. Appl. Crystallography* **45**, 1236 (2012).
- [21] Crystallography Open Data Base.
- [22] B. Domengès, F. Abbattista, C. Michel, M. Vallino, L. Barbey, N. Nguyen, and B. Raveau, *J. Solid State Chem.* **106**, 271 (1993).
- [23] M. Martínez-Ripoll, S. Martínez-Carrera, and S. García-Blanco, *Acta Crystallogr., Sect. B* **27**, 677 (1971).
- [24] E. N. Ovchinnikova *et al.*, *J. Synchrotron Radiat.* **28**, 1455 (2021).
- [25] O. Bunau and Y. Joly, *J. Phys.: Condens. Matter* **21**, 345501 (2009).
- [26] M. A. K. Ahmed, A. Kjekshus, and H. Fjellvag, *J. Chem. Soc. Dalton Trans.* **2000**, 4542 (2000).
- [27] S. H. Elder, F. J. DiSalvo, J. B. Parise, J. A. Hriljac, and J. W. Richardson, Jr., *J. Solid State Chem.* **108**, 73 (1994).
- [28] F. Abraham, J. Trehoux, and D. Thomas, *J. Inorg. Nuclear Chem.* **42**, 1627 (1980).
- [29] Q. Wu, X. Meng, C. Zhong, X. Chen, and J. Qin, *J. Am. Chem. Soc.* **136**, 5683 (2014).
- [30] L. Nian, J. Huang, K. Wu, Z. Su, Z. Yang, and S. Pan, *RSC Adv.* **7**, 29378 (2017).
- [31] W. Xing *et al.*, *J. Mater. Chem. C* **9**, 1062 (2021).